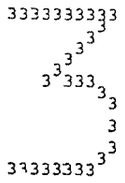

ISOBARIC ANALOG RESONANCE SPECTROSCOPY

In the experimental study of the fine structure excitation function for the reactions $^{55}Mn\ (p,n)^{55}Fe$ and $^{80}Se\ (p,n)^{80}Br$, several isobaric analog resonances (IARs), both old and new, have been observed. The present chapter deals with the analysis of these resonances to extract the relevant spectroscopic information. The mechanism of formation and decay of the IARs in proton induced reactions is discussed in the first two sections. The next section is devoted to a description of the methods used to derive information on Coulomb displacement energies between the isobaric pairs. The analytical tools to deduce the spectroscopic factor from experimental data and the results obtained for the prominent resonances seen in the present work are discussed in the last two sections.

3.1 ISOSPIN QUANTUM NUMBER

A fundamental feature of nuclear structure is associated with the presence of two kinds of nucleons, the neutron and the proton. The near equality of the masses of these particles immediately suggests a deep similarity between them and the more detailed study of their role in nuclear processes has revealed a basic symmetry between neutron and proton in all nuclear interactions. The nuclear forces are found to be charge independent to within a few percent.[1] This is expressed by defining an "isospin quantum number" $\vec{\tau}$, similar to the spin quantum number and having two states of the nucleon representing neutron ($\tau_z = +\frac{1}{2}$) and proton ($\tau_z = -\frac{1}{2}$). The nucleon wave function is then required to be anti-symmetric with respect to the interchange of space, spin and isospin quantum numbers.

For systems with two or more nucleons, the isospin may be coupled in the same way as angular momentum. Thus,

$$\vec{T} = \sum_i \vec{\tau}_i \qquad \ldots \qquad (3.1)$$

with the z-component $T_z = (N-Z)/2$, where N and Z are the number of neutrons and protons respectively.

The operator $\vec{T}$ can be associated with rotation in isospace in the same manner as the angular momentum $\vec{L}$ generates rotation in ordinary space. It can be proved that the assumption of charge independence leads to the rotational invariance in isospace. This further implies that the Hamiltonian of the system commutes with the total isospin T. The stationary states can thus be labelled with the quantum number T and the states form degenerate multiplets consisting of (2T+1) components with different T_z. Nuclear states described by the same set of space, spin and isospin quantum numbers and differing only in the z- component T_z of the isospin quantum number are called the Isobaric Analog States.

The isobaric invariance is violated by the electromagnetic interaction which lifts the degeneracy of the isobaric multiplet. The symmetry breaking effects in the nuclear structure are partly associated with the Coulomb force between the nucleons. For the lightest nuclei, these effects are small and mainly act to give small energy splitting between the isobaric multiplets. In heavier nuclei, however, the Coulomb field may become very strong, reaching values of the order of 20 MeV inside the heaviest nuclei. Thus for a long time it was believed that the isobaric symmetry might be of little significance in heavy nuclei. The discovery of well defined isobaric multiplet structure[6] has revealed , however, that the strong Coulomb interactions are rather ineffective in breaking the isobaric symmetry.

The validity of the T- quantum number in heavy nuclei may be understood from the fact that the Coulomb field varies rather slowly over the nuclear volume.[1] Thus the wave functions of the individual protons are only little affected and the main result of the Coulomb field is to add to the nuclear energy a term depending on the number of protons (i.e., on T_z) without violating the T- quantum number. For highly excited states, appreciable T- mixing must be expected since states of different isospin but same spin and parity occur close together and can be coupled by even relatively weak perturbations. In general, reactions proceeding through the formation of long lived intermediate states may thus involve appreciable isospin mixing.

3.2 FORMATION OF IARs IN PROTON INDUCED REACTIONS

In medium and heavy nuclei, the strong Coulomb interaction implies that the most stable nuclei with a given A have a large neutron excess and thus $T_z = (N-Z)/2$ is appreciably larger than unity. The isospin quantum number T must be equal to or greater than T_z and all the low lying energy levels

are found to have minimum isospin $T = T_0 = T_z$. The lowest states with $T = T_0+1$ in the target plus proton system, which are isobaric analogs of the low lying bound states of the target plus neutron system, occur at excitation energies well above the threshold for proton emission. These are often observed as sharp resonances in proton induced reactions on the same target.[35] The study of these isobaric analog resonances has provided an extensive body of evidence regarding the validity of isospin symmetry in heavier nuclei and also a new tool to study the spectroscopy of high lying states in the target plus proton system.

The formation of an IAR through proton induced reactions and its relation to the parent states is schematically illustrated in fig. (3.1) for the case of the reaction ^{55}Mn (p,n) ^{55}Fe. The symbols P, T, C and R denote respectively the parent (target plus neutron), target, compound (target plus proton) and the residual nuclei. It is assumed that the total isospin T for the ground state of these nuclei is the same as the respective T_z values. For the target nucleus, $T = T_z = T_0$ and it can be easily seen that the ground state isospins for the parent, compound and the residual nuclei respectively are $T_P = T_0+\frac{1}{2}$, $T_C = T_0-\frac{1}{2}$ and $T_R = T_0-1$. When a proton is added to the target with the ground state isospin T_0, the compound nuclear states can have isospins $T = T_< = T_0-\frac{1}{2}$ and $T = T_> = T_0+\frac{1}{2}$. The former are the normal compound nuclear states and the latter are the isobaric analogs of the states in the parent nucleus.

Fig. (3.1) also illustrates the energy relations between various states involved in the formation of an IAR in the reaction ^{55}Mn (p,n) ^{55}Fe. The energy difference between the parent and the analog states is

$$E_{T_>} - E_{T_<} = \Delta E_C - (n-H) = \Delta E_C - \delta \quad \ldots \quad (3.2)$$

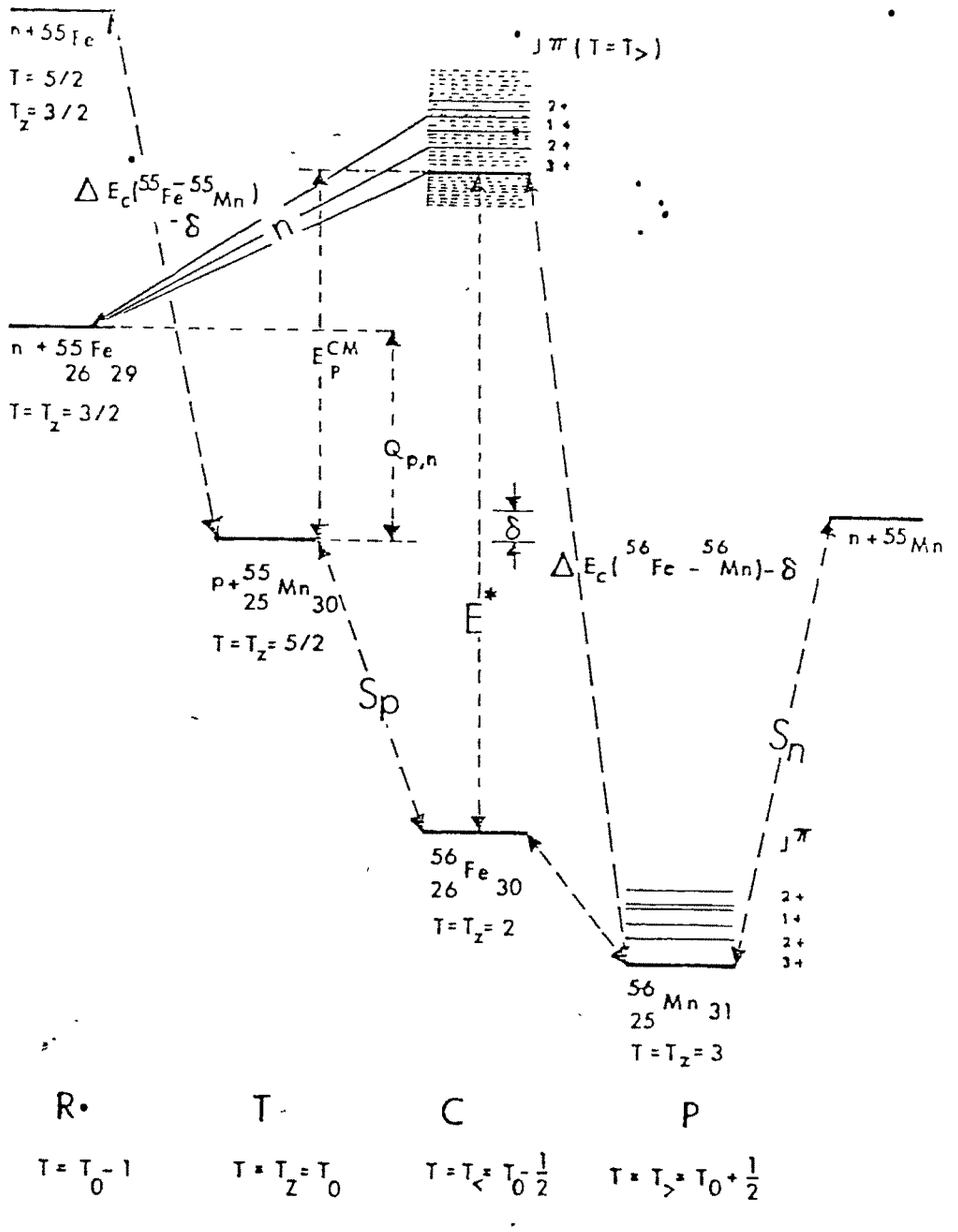

Fig. (3.1) Schematic representation of the various states involved and the energy relations in the formation and decay an IAR in the reaction ^{55}Mn (p,n) ^{55}Fe. The symbols P, C, T and R denote respectively the parent (target plus neutron), compound (target plus proton), target and residual nuclei. T_0 is the ground state isospin of the target.

Other energy relations evident from fig. (3.1) are :

$$E_p^{cm} = E^* - S_p \quad \ldots \quad (3.3)$$

where S_p is the proton separation energy, E^* is the excitation energy of the compound nucleus and E_p^{cm} is the centre-of-mass energy of the incident proton. Also, we have

$$\Delta E_c = S_n + E_p^{cm} \quad \ldots \quad (3.4)$$

where S_n is the neutron separation energy. Combining eqns. (3.3) and (3.4) we can write

$$E^* = \Delta E_c + (S_p - S_n) \quad \ldots \quad (3.5)$$

The structure around a resonance as seen in proton induced reactions can be represented by a smoothly varying direct amplitude and a Breit-Wigner type resonance amplitude.[7] Since the proton energies are several MeV below the Coulomb barrier, the direct amplitude is approximately equal to that given by the optical model potential. The elastic proton partial width Γ_p and the total width Γ can be deduced in various ways[29,36,51] from a shape analysis of the resonance.

The observed values of Γ_p may be compared with the single particle width Γ_p^{sp} that would be expected if the resonance could be described in terms of single particle motion. The states in ^{56}Mn would then correspond to a single neutron moving in the potential of the target nucleus ^{55}Mn in its ground state, while the isobaric analog state in ^{56}Fe would be represented by

$$|T=T_0+\tfrac{1}{2},\ T_z=T_0-\tfrac{1}{2}\rangle = \left(\frac{1}{2T_0+1}\right)^{\frac{1}{2}} |p;\ T_0, T_z=T_0\rangle + \left(\frac{2T_0}{2T_0+1}\right)^{\frac{1}{2}} |n;\ T_0, T_z=T_0-1\rangle \quad \ldots \quad (3.6)$$

This state is a linear superposition of the proton plus target (^{56}Fe) and neutron plus target analog (lowest $T=T_0$ state in ^{55}Fe).

The Coulomb field implies that the state represented by eqn. (3.6) is coupled to the normal compound nuclear state having the same single particle configuration and $T = T_0 - \frac{1}{2}$ as

$$|T=T_0-\tfrac{1}{2},\ T_z=T_0-\tfrac{1}{2}\rangle = \left(\frac{2T_0}{2T_0+1}\right)^{\frac{1}{2}} |p;\ T_0, T_z=T_0\rangle - \left(\frac{1}{2T_0+1}\right)^{\frac{1}{2}} |n;\ T_0, T_z=T_0-1\rangle \quad \ldots\ (3.7)$$

A striking consequence of the Coulomb interaction is the fact that the proton channel is open while the neutron channel is closed, the proton energy is below the (p,n) reaction threshold exciting the analog state of the target as can be seen from fig. (3.1). The neutron decay of the analog state in the compound nucleus to one of the normal states of the residual nucleus is isospin forbidden. This asymmetry between the proton and the neutron channel implies a major coupling of the states represented by eqns. (3.6) and (3.7) when the nucleon is outside the nucleus[7] (external mixing as discussed by Robson). The dense spectrum of $T_<$ $(=T_0-\frac{1}{2})$ levels is expected to have great complexity and one may describe the T- violating coupling as a decay of the $T_>$ $(=T_0+\frac{1}{2})$ levels with the formation of a compound nucleus in the $T_0-\frac{1}{2}$ channel having the same spin and space quantum numbers. Because of the Coulomb barrier, compound nucleus decays primarily by neutron emission and the observed resonances in (p,n) reactions may be interpreted in this manner.

The ratio between the observed Γ_p and the single particle value provides a measure of the spectroscopic factor of the single particle state and can be compared with the spectroscopic factors observed in the neutron transfer reaction ^{55}Mn (d,p)^{56}Mn populating the $T_z = T_0+\frac{1}{2}$ components of the $T = T_> = T_0+\frac{1}{2}$ states. The correspondence between these two provides further tests of the states as members of the T- multiplet.

3.3 COULOMB DISPLACEMENT ENERGY

The binding energy difference between the isobaric analog states is essentially given by the Coulomb energy. Thus all experimental studies of IARs also yield numerical values for the Coulomb displacement energy ΔE_c as is evident from fig. (3.1) and eqn. (3.4). The major objectives for studying

Coulomb energy are : (i) to obtain an understanding of the dependence of Coulomb energies on Z and A for a larger group of nuclei or to investigate its dependence on the detailed nuclear structure for a smaller group of nuclei; (ii) to obtain information about the charge distribution and the charge radii of atomic nuclei and (iii) to understand the importance of the violation of charge independence of nuclear forces, if any.[30]

The ΔE_c values obtained in the present investigation of IARs in the reactions ^{55}Mn (p,n) ^{55}Fe and ^{80}Se (p,n) ^{80}Br are listed in Table 3.1 for different sets of excited patent and analog states in the isobaric pairs ^{56}Mn - ^{56}Fe and ^{81}Se - ^{81}Br. One expects small variations in the Coulomb energy

TABLE 3.1

Coulomb Displacement Energies

E_p^{cm} (MeV)	E_x (MeV)	B_n (MeV)	ΔE_c (MeV)	$\langle \Delta E_c \rangle$ (MeV)	R_c (fm)**
		^{56}Fe - ^{56}Mn			
1.365	0.026	7.244	8.609		
1.430	0.110	7.160	8.590	8.583 ± 0.025	1.262
1.515	0.214	7.506	8.571		
3.546	2.254	5.016	8.562		
		^{81}Br - ^{81}Se			
3.785	0.0	6.714	10.499		
4.267	0.469	6.245	10.512		
4.813	1.053	5.661	10.474	10.478 ± 0.035	1.252
4.956	1.234	5.480	10.436		
5.032	1.304	5.410	10.442		
5.198	1.407	5.307	10.505		

** calculated using equations (3.9) and (3.10)

shifts for the different $T_>$ states, depending on the intrinsic structure of the levels.[1] The observed variations are quite small (less than 30 keV) and this may be understood from the fact that the Coulomb energy difference represents the average Coulomb energy for the proton states obtained by replacing one of the six different excess neutrons of ^{56}Mn (and similarly for ^{81}Se) by a proton. Since the different levels in ^{56}Mn differ primarily in the orbits of a single or a few nucleons, the energy shift is expected to vary only a little from level to level.[1]

In a quantal description of Coulomb energy one must take into account the correlation of protons that is implied by the anti-symmetrization of the wave function. Considering the estimate of this effect, one finds that for a heavy nucleus in the uniform density model and using plane waves for the proton wave function[1,47]

$$E_c \approx \frac{3}{5} \frac{Z^2 e^2}{R_c'} \left(1 - 0.767\, Z^{-2/3} \right) \quad \ldots \quad (3.8)$$

where R_c' is the radius of the uniform charge density. For a Fermi distribution of diffuseness a, the above equation is modified to

$$E_c \approx \frac{3}{5} \frac{Z^2 e^2}{R_c} \left(1 - 0.767\, Z^{-2/3} \right) \left(1 - \frac{7}{6} \frac{\pi^2 a^2}{R_c^2} + \ldots \right) \quad \ldots \quad (3.9)$$

where R_c is the half value radius. The Coulomb energy difference ΔE_c between the isobars (Z+1, A) and (Z, A) can be deduced using the above relation as

$$\Delta E_c = E_c(Z+1, A) - E_c(Z, A) \quad \ldots \quad (3.10)$$

A general form for the Coulomb energy difference between analog states of nuclei (Z+1, A) and (Z, A) as suggested by Sengupta[48] is

$$\Delta E_c = \frac{e^2}{R_c A^{1/3}} \left\{ \frac{3}{5} (2Z + 1) - 0.613\, Z^{1/3} - 0.30\, (-1)^Z \right\} \quad \ldots \quad (3.11)$$

The last term corresponds to the change in pairing effects of proton spins on the exchange contribution in the above formula (3.11).

The ΔE_c values extracted from experimental data show significant pairing and shell effects. In this connection, it is important to examine the validity of extracting ΔE_c from an expression derived for the average behaviour of protons within a nucleus. In β-decay, (p,n) analog reactions and in fact whatever source is used in determining ΔE_c, protons predominantly in a specific orbital state are involved. Thus changes in Coulomb energy should be calculated for such protons alone rather than the average proton state. An important difference also arises from the model sensitivity of the treatment of the exchange energy contribution to ΔE_c for isobaric analogs, particularly for light nuclei.

An empirical expression for ΔE_c taking the shell and pairing effects into account, with an accuracy of 15 keV in the range $48 \leq A \leq 208$ has been developed by Seitz et al.[49] Consideration has been given to magic and isotopic effects as well as nuclear deformation. The resulting expression is:

$$\Delta E_c(Z+1,Z) = \frac{E_1 Z}{A^{1/3}} \left(1 - \frac{4}{45}\delta^2\right) + E_2 + \{1 - (-1)^Z\} \frac{60}{N-Z} - \frac{86Z}{A\,t} \qquad (3.12)$$

with $E_1 = (1.3941 \pm 0.003)$ MeV, $E_2 = (-0.416 \pm 0.040)$ MeV, δ is a suitably defined deformation parameter and t is the average of $\vec{l}.\vec{\sigma}$ over (2T+1) neutron orbitals that constitute the analog state in a shell model description. The third term results from the Coulomb pairing interaction and is zero except for odd-Z nuclei. The last term is a Coulomb spin-orbit interaction and is generally within 40 keV. The deformation parameter δ reaches a peak value of ≈ 0.3 in the mid-earth region.

The expressions (3.10) to (3.12) can also be used to determine the radius parameter using the experimentally observed values of the Coulomb energy difference.[37,38] The value of r_c (where $R_c = r_c.A^{1/3}$) obtained in the present case is shown in Table 3.1 and is found to be slighly larger than the values obtained from electron scattering data. Such a difference

may be expected from the fact that the isobaric displacement energy represents the Coulomb energy of an extra charge having a radial density distribution corresponding to that of the excess neutrons; these neutrons have somewhat larger radii than the total proton distribution.

Coulomb energies also yield information on the difference of rms radii of neutron and proton density distributions, $\Delta = \langle r_n^2 \rangle^{\frac{1}{2}} - \langle r_p^2 \rangle^{\frac{1}{2}}$. While the inferred results are model sensitive , the values suggest that

Δ = (0.05 to 0.15) fm.[50]

3.4 EXTRACTION OF NEUTRON SPECTROSCOPIC FACTOR

3.4.1 Shape Analysis of the Resonance

At sub-Coulomb energies the isobaric analog resonances can be analysed using the simple procedure of Breit-Wigner (BW) resonances.[39] For resonances superimposed over a background amplitude, the BW expression is written as

$$\sigma_p^{tot}(E) = \sigma_p'(tot) + \pi \lambda^2 g_J \frac{\Gamma_p . W}{(E-E_0)^2 + \frac{1}{4}(\Gamma_p + W)^2} \quad \ldots \quad (3.13)$$

where Γ_p is the proton partial width and W accounts for the widths in all the outgoing channels and is identified with the "spreading width" of the Coulomb perturbation. In the above expression, E_0 is the energy of the resonance, $\sigma_p'(tot)$ is the total background reaction cross section and other symbols have their usual meaning. For IARs observed in (p,n) excitation functions, $W \approx \Gamma_n$ and neglecting other channels of very small partial widths, the total width $\Gamma = \Gamma_p + \Gamma_n$. However, eqn. (3.13) allows only the determination of the product $\Gamma_p . \Gamma_n$ and specific assumptions about the relative values of Γ_p and Γ_n must be made to determine Γ_p.

Proton partial width Γ_p can be unambiguously determined from the detailed shape analysis of the resonance structure according to the formalism developed by Robson based on R-matrix theory.[7] Two major assumptions are made - (i) a single proton channel needs to be considered, and (ii) there is negligible mixing in the interior i.e., isospin is a good quantum number inside and Coulomb mixing occurs externally to the extent which depends on the choice of boundary conditions. With the additional assumption that direct reaction contributions are negligible at sub-Coulomb energies and that proton re-emission can be neglected, the expression for the shape of the IAR can be written as[36]

$$\sigma_{pn}^{res} = \sigma'_{pn}(bkg) \left\{ \frac{(E - E_J + \Delta)^2}{(E - E_0)^2 + \Gamma_0^2/4} - 1 \right\} \quad \ldots \quad (3.14)$$

Eqn. (3.14) will henceforth be referred to as Robson-Johnson (RJ) formalism. In the above equation E_0, Δ and Γ_0 are respectively the energy, level shift and the total width of the resonance. The background cross section $\sigma'_{pn}(bkg) = \pi \lambda^2 g_J T'_p$, where T'_p is the non-resonant transmission factor that would exist if the resonance were absent and it can be calculated using the optical model. Having determined Δ from a shape analysis of the resonance using eqn. (3.14), the proton partial width Γ_p can be calculated from the relation[7]

$$2\Delta/\Gamma_p = -(S_{p^*} - B_c) / P_{p^*} \quad \ldots \quad (3.15)$$

where S_{p^*}, B_c and P_{p^*} are the shift factor, boundary condition parameter and the penetrability in the usual terminology of R-matrix theory.[40] The spreading width W may then be extracted from the relation

$$W = \pi s_{p^*} (S_{p^*} - B_c)^2 \Gamma_p / P_{p^*} \quad \ldots \quad (3.16)$$

where s_{p^*} is the proton strength function.

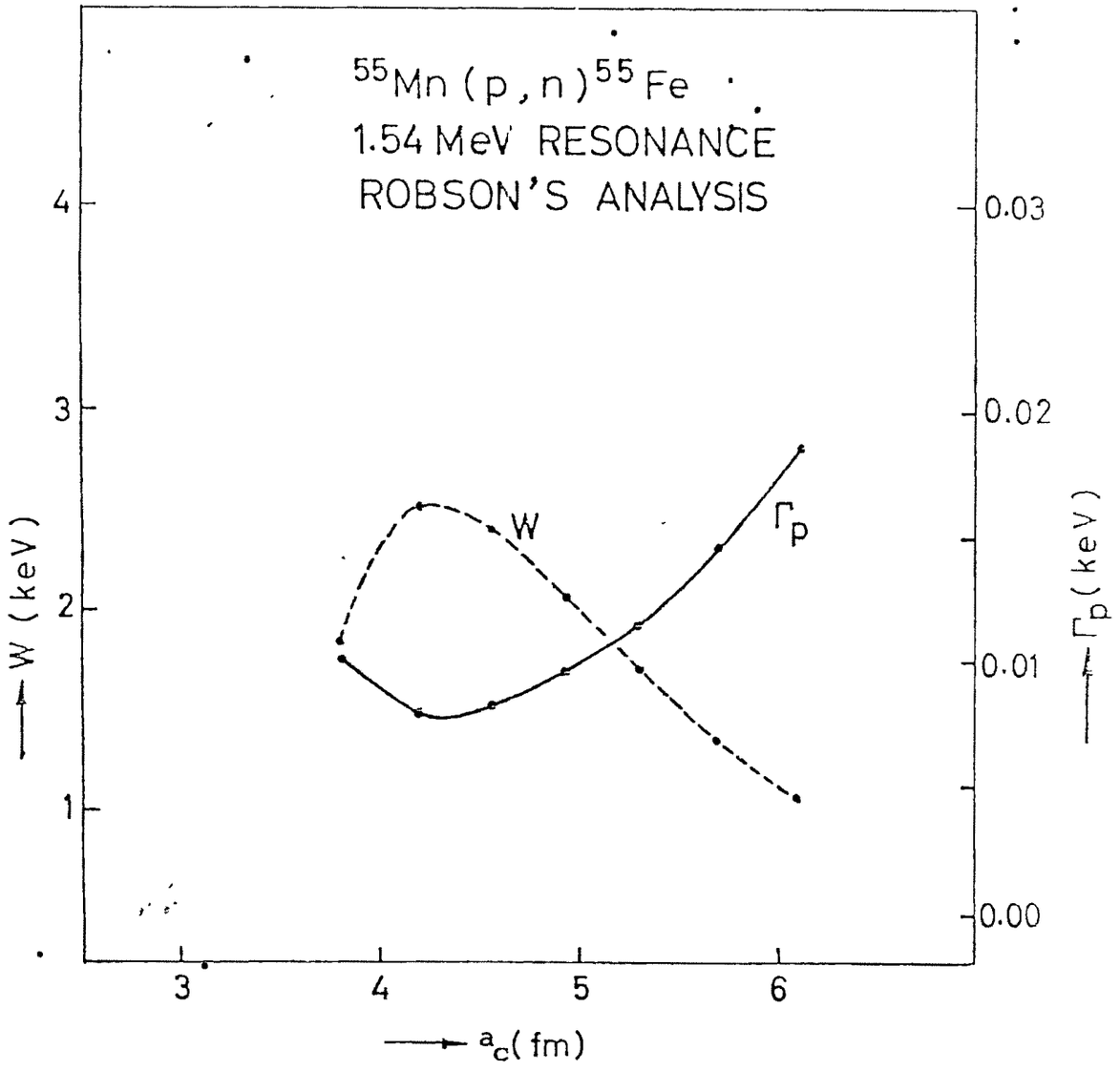

Fig. (3.2) Variation of Γ_p and W as a function of channel radius.

The quantities S_{p*} , B_c and P_{p*} of the R-matrix theory are functions of the channel radius a_c. This leads to a variation of Γ_p with a_c. In orde to study this variation detailed calculation of Γ_p and W for various valuc of the channel radius have been performed over physically meaningful range. A plot of Γ_p and W as a function of a_c is shown in fig. (3.2) for the case of 1.54 MeV resonance in ^{55}Mn (p,n) ^{55}Fe reaction. The extremum values of Γ_p and W for the calculation of the spectroscopic factor are obtained by requiring that

$$\frac{\partial \Gamma_p}{\partial a_c} = 0 \quad ; \quad \frac{\partial W}{\partial a_c} = 0 \qquad \ldots \qquad (3.17)$$

The shape analysis of the IARs observed in both $^{55}Mn\ (p,n)^{55}Fe$ and $^{80}Se\ (p,n)^{80}Br$ reactions have been done using the above procedure and the results are presented in Table 3.2. The background cross section $\sigma'_p(bkg)$ was treated as a free parameter for fitting with eqns. (3.13) and (3.14). The fits are shown in figs. (3.3) and (3.4). For the 1.54 MeV resonance in the case of $^{55}Mn\ (p,n)^{55}Fe$ reaction, the two values of the partial widths obtained by fitting with a BW shape are also shown in Table 3.2.

TABLE 3.2

Shape Parameters of the IARs

E_0 (MeV)	Γ_0 (keV)	$\lvert\Delta\rvert$ (keV)	Γ_p (keV)	W (keV)	$\sigma'_p(bkg)$ (mb)
		$^{55}Mn\ (p,n)^{55}Fe$			
1.543	3.3 ± 0.1	22 ± 0.6	0.0078 ± .0001	2.5 ± .03	0.1
	(3.4)*		(0.0075 ± .0002)	(3.4 ± .06)	
		$^{80}Se\ (p,n)^{80}Br$			
3.785	18.0 ± 1.0	33 ± 2	2.3 ± 0.1	9.9 ± 0.6	3.5
4.267	12.0 ± 3.0	6 ± 1	0.8 ± 0.1	2.9 ± 0.5	19.0
4.813	11.0 ± 1.0	11 ± 1	1.3 ± 0.1	6.1 ± 0.6	26.0
4.956	36.0 ± 7.0	19 ± 2	8.1 ± 0.9	14.7 ± 1.5	44.0
5.032	31.0 ± 1.0	26 ± 2	3.8 ± 0.3	14.2 ± 1.1	32.0
5.198	27.0 ± 8.0	7.5± 2.9	2.7 ± 0.1	4.6 ± 1.8	53.0

* numbers in parentheses are the results of BW analysis for this resonance.

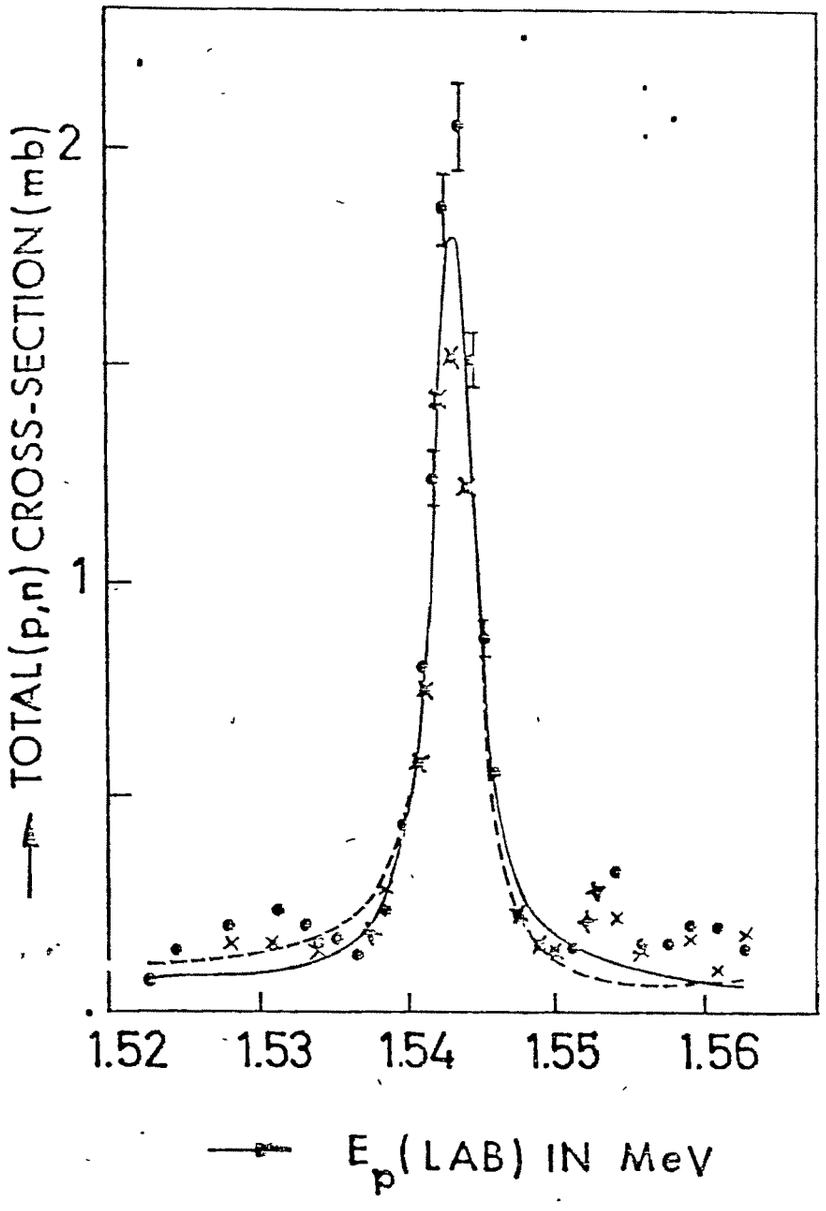

Fig. (3.3) Shape analysis of the IAR at E_p = 1.543 MeV measured with ~ 1 keV thick target. The dots and crosses represent two separate runs over the resonance. The continuous curve is the fit to the data with BW formula with E_0= 1.543 MeV and Γ_0=3.4 keV. The dashed curve is a fit to the data with RJ formula with Δ =-22 keV, σ'_p(bkg) = 0.1 mb, E_0= 1.543 MeV and Γ_0=3.3 keV.

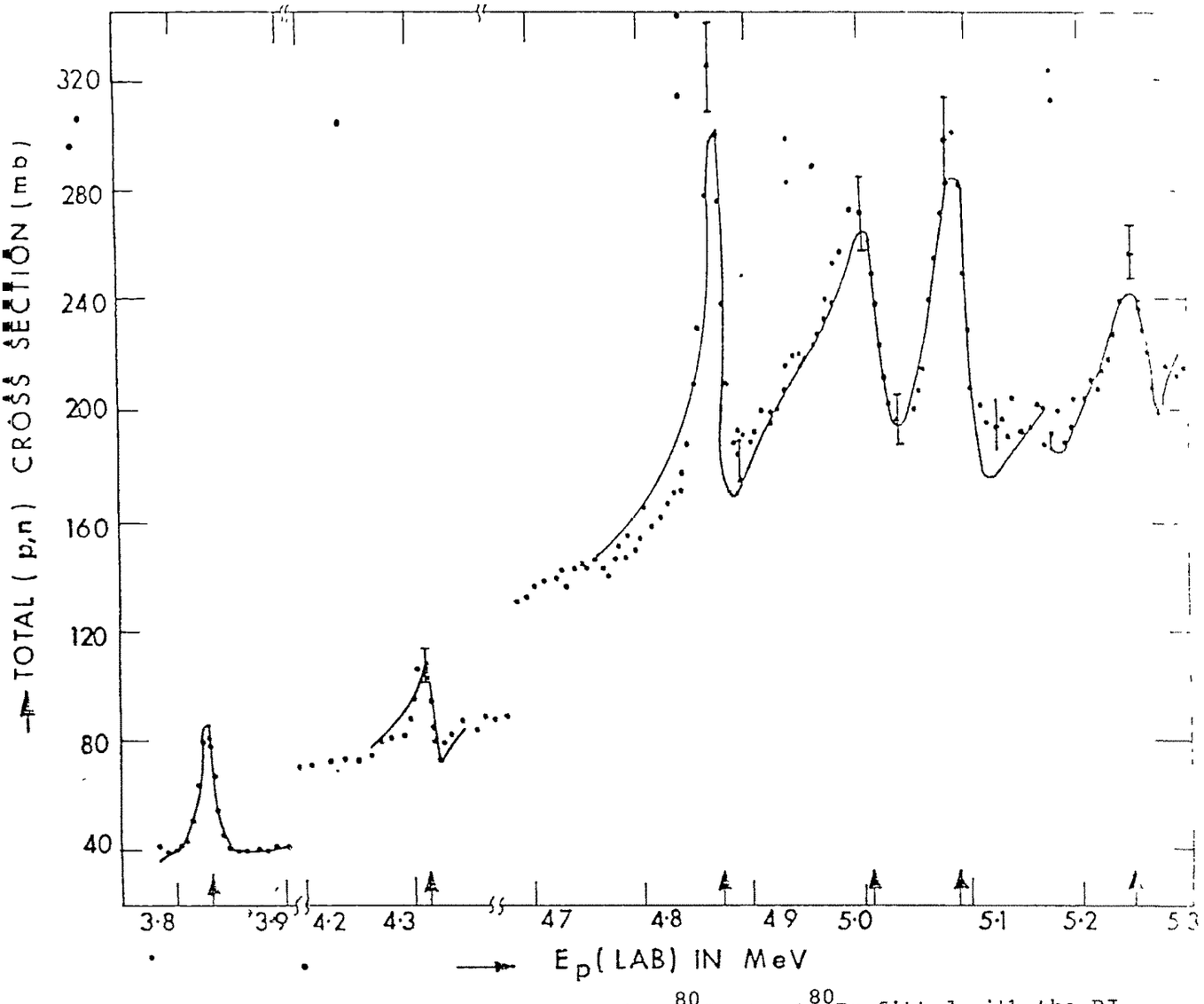

Fig. (3.4) IARs in the reaction ^{80}Se (p,n) ^{80}Br fitted with the RJ formula (continuous curve). The parameters are listed in Table 3.2.

It is found that the value of Γ_p extracted from RJ formulation for the 1.54 MeV resonance is very close to the smaller value of the two partial widths obtained from the BW analysis. The larger of the partial widths in BW analysis is of the order of spreading width W as is to be expected. A combination of these two methods of analyses of IARs thus allows us to extract an unambiguous value of Γ_p for the calculation of spectroscopic factors.

The errors quoted on the values of Γ_p and W in Table 3.2 are those determined from the fitting procedure and reflect the scatter of points (i.e., statistical and other uncertainties due to the non-uniformity of the target and small beam energy fluctuations). The absolute errors on these quantities, however, would have a maximum value of 15% reflecting the absolute error in the cross section measurements.

3.4.2 Spectroscopic Factor

The simple relation between states belonging to the same isobaric spin multiplet suggests that there is also a simple relation between the resonances observed in proton induced reactions and the corresponding states seen in neutron capture via (d,p) stripping on the same target nucleus. Information gained by observing analog resonances in proton induced reactions is essentially equivalent to the information gained from (d,p) stripping, so that proton reactions via analog states constitute an alternative method for nuclear spectroscopic studies.

The spectroscopic factor S_n for the neutron single particle state in the parent nucleus is defined as[41]

$$S_n = \gamma_n^2 / \gamma_{sn}^2 \quad \ldots \quad (3.18)$$

where γ_{sn}^2 is the neutron single particle reduced width and γ_n^2 is the experimental neutron reduced width. The latter is obtained from Γ_p using the following relations[41]

$$\gamma_n^2 = \gamma_p^2 (2T_0+1) \; ; \quad \gamma_p^2 = 2 P \Gamma_p \quad \ldots \quad (3.19)$$

where P is the usual Coulomb penetrability and γ_p^2 is the proton reduced width. The neutron single particle reduced width γ_{sn}^2 is calculated using the bound state neutron wave function[41]

$$\gamma_{sn}^2 = \frac{\hbar^2}{2 M a_c} \frac{U_n^2(a_c)}{\int_0^{a_c} |U_n^2(r)| \, dr} \quad \ldots \quad (3.20)$$

where $U_n(r)$ is the radial neutron wave function for a single particle state at the energy of the parent analog, M is the neutron mass and a_c is the channel radius. It is thus obvious that the calculation of S_n using eqn. (3.18) requires, in addition to Γ_p, the proton plus target and neutron plus target optical model parameters and the proton channel radius a_c.

The computer computer code SSEARCH[42] has been used to extract the neutron spectroscopic factor S_n from experimental values of proton partial widths and these have been compared with the spectroscopic factors obtained from (d,p) reactions as available in literature. The parameters of the optical model potential (OMP) used in the calculation are listed in Table 3.3 for both the targets studied, the symbols have their usual meanings. In the discussions to follow, the geometrical parameters of the neutron OMP will be referred to as r_{n0} (the radius parameter) and a_n (the diffuseness) for the sake of brevity. As the neutron OMP is needed only for bound state calculations, imaginary potential has not been included and the depth of the real neutron OMP has been adjusted to reproduce the binding energy of the given state in the parent nucleus.

TABLE 3.3

OMP Parameters for the Calculation of S_n

Target	V	r_v	a_v	W	r_w	a_w	V_{so}	r_{so}	a_{so}
				Proton					
^{55}Mn	58.0	1.175	0.65	5.0	1.32	0.574	6.0	1.12	0.65
^{80}Se	58.0	1.25	0.65	5.0	1.25	0.47	7.5	1.25	0.65
				Neutron					
^{55}Mn	...	...	(all varied)**		...		...	...	
^{80}Se	-	1.25	0.65	-	-	-	7.5	1.25	0.65

** see discussion on parameter variation of S_n

3.5 RESULTS AND DISCUSSIONS

3.5.1 IARs in ^{55}Mn (p,n)^{55}Fe Reaction

The IAR observed in the (p,n) excitation function at E_p^{cm} = 1.54 MeV has been analysed in detail to study the parameter dependence of the extracted S_n. It is found to be quite sensitive particularly to changes in the geometrical parameters of the real part of the neutron OMP and also to changes in the channel radius a_c. In order to study the sensitivity, S_n values have been calculated for a set of r_{n0} and a_n values in the following way : For each value of r_{n0} and a_n the spectroscopic factor S_n was calculated as a function of a_c. In general S_n is expected to go through a minimum as a function of a_c.[41] It was found that this was not true for some r_{n0} values. However, in all cases the S_n vs. a_c curve exhibited a plateau as shown in fig. (3.5), where the value of S_n became insensitive to variations in a_c. This value of S_n (corresponding to a_c = 6.4 fm in the present case) was chosen as an indicative value to study its variations with r_{n0} and a_n. Results of these calculations are shown as curves numbered (3) and (4) in fig. (3.6). Other calculational details are given in the figure caption. This investigation clearly indicates strong dependence of S_n on r_{n0} and a_n. The S_n values were found to be almost insensitive to the proton OMP parameters.

The spectroscopic factor obtained from the (d,p) reaction studies is also similarly dependent on neutron potential parameters.[43] The experimental data of Comfort[31] for the reaction ^{55}Mn (d,p)^{56}Mn pertaining to the 0.213 MeV state has been reanalysed for the present purpose using his potential parameters and the computer code DUWK to obtain neutron spectroscopic factors for the parent state for various values of r_{n0}. The variation of this S_n (called S_{DP}) with r_{n0} is shown as curve numbered (1) in fig. (3.6) and can be compared with S_{PN} (derived from the present (p,n) study) to judge the relation between the two spectroscopic factors.

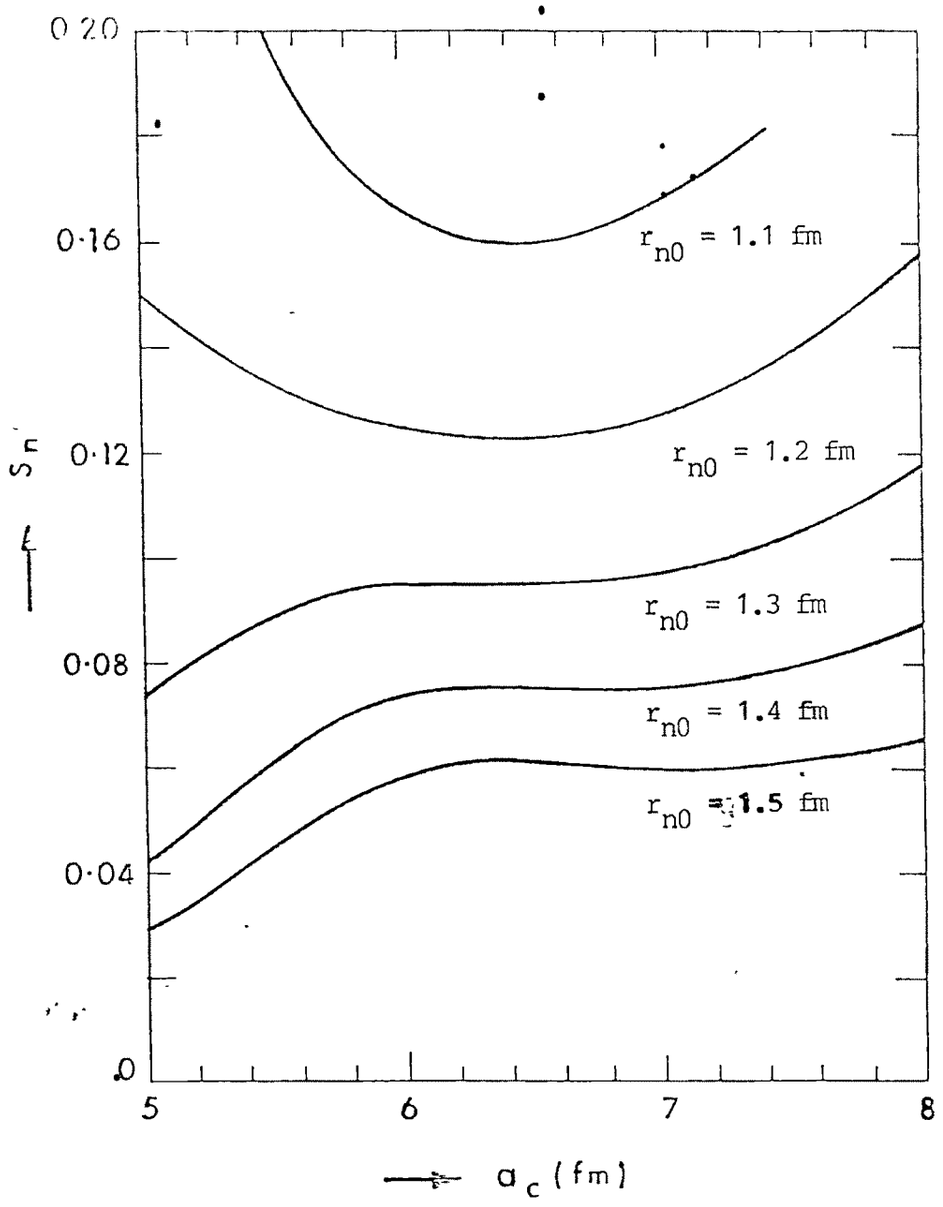

Fig. (3.5) Variation of neutron spectroscopic factor as a function of channel radius a_c for various values of the radius parameter r_{n0} of the real neutron OMP. Other parameters of the proton OMP used to calculate S_n were the same as listed in Table 3.3 . For neutron, the depth V = 59.4 MeV and diffuseness a_n = 0.7 fm were used.

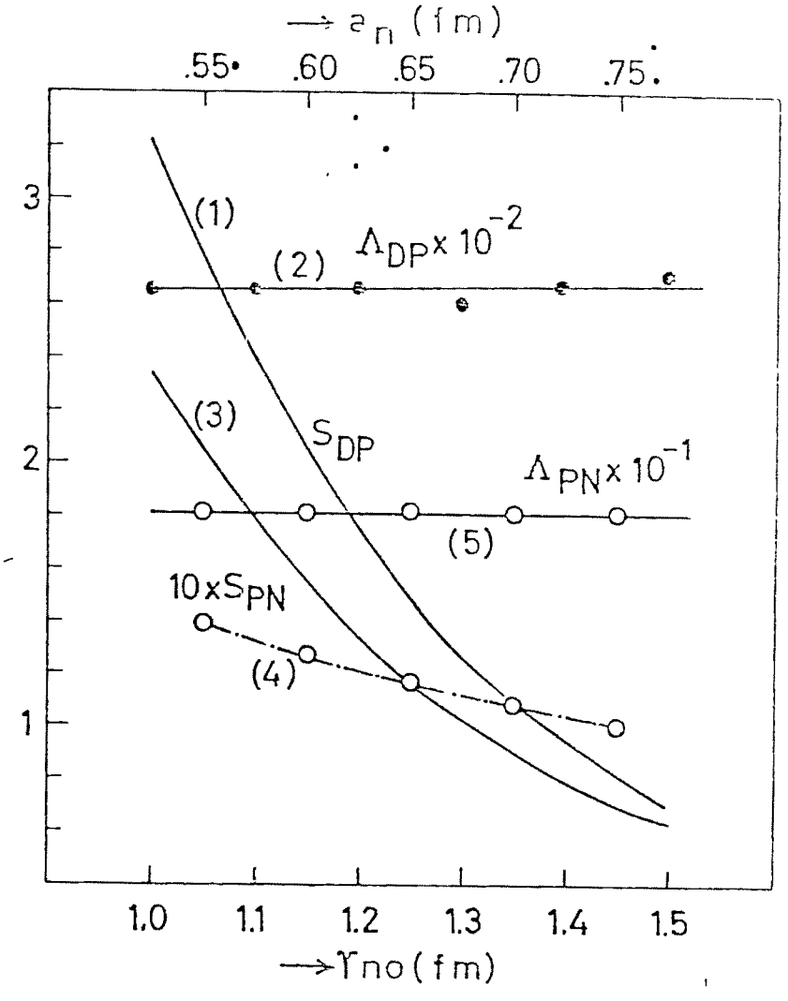

Fig. (3.6) Variation of spectroscopic factor S and reduced normalization Λ with r_{n0} and a_n. Curves numbered (1) and (2), respectively, show the variation of S_{DP} and Λ_{DP} as a function of neutron radius parameter r_{n0} (a_n being fixed at 0.65 fm). Curves numbered (3) and (4) respectively, show the variation of S_{PN} with r_{n0} (a_n = 0.65 fm) and with a_n (r_{n0} fixed at 1.25 fm). Curve numbered (5) gives the variation of Λ_{PN} with r_{n0} (a_n fixed at 0.65 fm). The subscripts DP and PN refer to the spectroscopic factor extracted from (d,p) and (p,n) data, respectively.

Comparison between the spectroscopic factors extracted from (d,p) and IAR data is done in a better way by using the "Reduced Normalization" Λ which is found to be less sensitive to parameter variations.[43,44] The quantity Λ has been obtained in the present work following the method of Clarkson et al[44] where it is defined as

$$\Lambda = S_n \left| U_n^2(r) \right| \quad \ldots \quad (3.21)$$

Harney and Weidenmuller have shown[45] that $\left| U_n^2(r) \right| . S_n$ (U_n being the normalized bound state wave function for neutron) is independent of neutron well parameters at a radius $r = a_c$ where the proton wave function is zero. Eqn. (3.21) is then modified to

$$\Lambda = S_n \left| U_n^2(a_c) \right| \quad \ldots . \quad (3.22)$$

In the present investigation, this value of a_c is again chosen at 6.4 fm where S_n as a function of a_c shows a plateau as discussed earlier. The Λ values calculated by the above procedure are also shown in fig. (3.6). It is found that the Λ_{PN} value is constant to within 1%. Similar calculations have been done for the (d,p) data as well and in this case the value of Λ_{DP} is found to be constant to within 4%.

The above detailed discussion would indicate the difficulties in comparing the results of (d,p) and (p,n) analyses of the single particle states due to the parameter dependence of S_n. The usefulness of the reduced normalization Λ in this regard is demonstrated. However, a comparison between the corresponding numbers in the present case shows that the values of optimum S_n as well as Λ obtained in the present (p,n) analysis (S_{PN} and Λ_{PN}) are lower by almost an order of magnitude compared with the corresponding values obtained from (d,p) studies. The disagreement upto a factor of 5 has been observed in such comparisons.[46] On the other hand, due to the fact that the (d,p) reaction study has not been able to resolve the doublet around the 0.215 MeV state (as discussed in sec. 2.6.1), the

spectroscopic factor obtained in that work would represent the combined strength of the two levels, while the present (p,n) study only measures the spectroscopic strength of the 0.215 MeV 2^+ level (the 4^+ level not being excited). In a study of the $^{55}Mn\ (n,\gamma)^{56}Mn$ reaction, Van Assche et al[32] have estimated the contribution from the two states and found only 40% being contributed by the 2^+ state. This would indicate a reduction in the value of S_{DP} for the 0.215 MeV state and thus would be in the right direction to be consistent with the (p,n) results.

3.5.2 IARs in $^{80}Se\ (p,n)^{80}Br$ Reaction

Using the above procedure, S_n has been calculated from the proton partial widths using a value of the channel radius $a_c \approx 6.0$ fm and the optical model parameters listed in Table 3.3. The S_n values obtained for the states in ^{81}Se in the present study along with those obtained from (d,p) and p,p) reaction studies are compared in Table 3.4 for the six IARs. It is evident that, in general, the S_n values extracted from the various works are comparable. However, for the IARs much below the Coulomb barrier, the S_n determined from the present (p,n) work agrees better with those of (d,p) measurements, whereas (p,p) work gives values widely different from the (d,p) studies. As the large Coulomb cross section at these energies makes the IAR an weak anomaly in the (p,p) excitation function, the determination of Γ_p may have large errors. This point is well illustrated by the weaker IAR around 4.2 MeV which is not observed at all in the (p,p) excitation function,[16] but which appears as a measurable resonance in the present work as seen clearly in fig. (3.4) and which could be subjected to detailed shape analysis for the extraction of spectroscopic factors.

TABLE 3.4

Comparison of the Spectroscopic Factors, Obtained from (p,n), (p,p) and (d,p) works on ^{80}Se

E_p^{cm} (MeV)	S_{pn} (*)	S_{dp} (17)	S_{pp} (16)
3.785	0.22	0.30	0.09
4.267	0.026	0.045	-
4.813	0.15	0.26	0.18
4.956	0.32	0.64	0.85
5.032	0.32	0.40	0.41
5.198	0.022	0.075	-

(*) present work

It must be mentioned here that unlike the case of 1.54 MeV resonance in ^{55}Mn (p,n) ^{55}Fe reaction, all the resonances in ^{80}Se (p,n) ^{80}Br reaction observed in the present experimental investigation correspond to well separated states in ^{81}Se and the extracted spectroscopic factors are free from the ambiguities arising from contributions from neighbouring states. This is the reason why the spectroscopic factors in the (p,n) and (d,p) studies agree so well. This agreement goes one step further to establish the hypothesis of the charge independence of nuclear forces.